MOLECULAR AND CELLULAR BIOLOGY, Dec. 2002, p. 8709–8720 Vol. 22, No. 24
0270-7306/02/$04.00+0 DOI: 10.1128/MCB.22.24.8709–8720.2002

CYR61 (CCN1) Is Essential for Placental Development and Vascular Integrity

Fan-E Mo,[1] Andrew G. Muntean,[1] Chih-Chiun Chen,[1] Donna B. Stolz,[2] Simon C. Watkins,[2] and Lester F. Lau[1]*

Department of Molecular Genetics, University of Illinois at Chicago, Chicago, Illinois 60607-7170,[1] and Center for Biologic Imaging, University of Pittsburgh, Pittsburgh, Pennsylvania 15261[2]

Received 14 June 2002/Returned for modification 31 July 2002/Accepted 25 September 2002

CYR61 (CCN1) is a member of the CCN family of secreted matricellular proteins that includes connective tissue growth factor (CCN2), NOV (CCN3), WISP-1 (CCN4), WISP-2 (CCN5), and WISP-3 (CCN6). First identified as the product of a growth factor-inducible immediate-early gene, CYR61 is an extracellular matrix-associated angiogenic inducer that functions as a ligand of integrin receptors to promote cell adhesion, migration, and proliferation. Aberrant expression of *Cyr61* is associated with breast cancer, wound healing, and vascular diseases such as atherosclerosis and restenosis. To understand the functions of CYR61 during development, we have disrupted the *Cyr61* gene in mice. We show here that *Cyr61*-null mice suffer embryonic death: ~30% succumbed to a failure in chorioallantoic fusion, and the reminder perished due to placental vascular insufficiency and compromised vessel integrity. These findings establish CYR61 as a novel and essential regulator of vascular development. CYR61 deficiency results in a specific defect in vessel bifurcation (nonsprouting angiogenesis) at the chorioallantoic junction, leading to an undervascularization of the placenta without affecting differentiation of the labyrinthine syncytiotrophoblasts. This unique phenotype is correlated with impaired *Vegf-C* expression in the allantoic mesoderm, suggesting that CYR61-regulated expression of *Vegf-C* plays a role in vessel bifurcation. The genetic and molecular basis of vessel bifurcation is presently unknown, and these findings provide new insight into this aspect of angiogenesis.

Development of the vascular system during embryogenesis occurs in two distinct processes: vasculogenesis, the formation of blood vessels in situ from angioblasts, and angiogenesis, the formation of blood vessels by sprouting from preexisting ones (38, 50). Successful vessel formation requires the orchestrated execution of multiple cellular processes—including the migration, proliferation, differentiation, and tube formation of vascular cells—that are coordinated with remodeling of the extracellular matrix (ECM). Many aspects of these processes are in turn subject to regulation by components of the ECM (44).

CYR61 (CCN1) is a novel ECM-associated angiogenic regulator of the CCN family, sharing a ~40 to 50% amino acid sequence homology with connective-tissue growth factor (CTGF) (CCN2), NOV (CCN3), WISP-1 (CCN4), WISP-2 (CCN5), and WISP-3 (CCN6) (7, 32, 37). Both CYR61 and CTGF are encoded by growth factor-inducible immediate-early genes, which are rapidly activated at the transcriptional level when responsive cells are stimulated with serum growth factors such as fibroblast growth factor, platelet-derived growth factor, and tumor transforming growth factor β (31, 36, 40). CCN proteins are organized into four conserved modular domains that share sequence similarities with insulin-like growth factor-binding proteins (IGFBPs), the von Willebrand factor type C repeat, the thrombospondin type 1 repeat, and the carboxyl termini of several extracellular mosaic proteins such as mucins and *slit* (5). The prominent structural similarities to ECM components suggest that CCN proteins resemble the functionally diverse matricellular proteins, which are also characterized by a mosaic of matrix protein domains (6). Despite discernible sequence similarity to IGFBPs, CYR61 is unlikely to bind insulin-like growth factor, since the specific residues in IGFBPs that interact with insulin-like growth factor are not conserved in CCN proteins (23, 25).

A cysteine-rich, secreted heparin-binding protein, CYR61 mediates cell adhesion, stimulates cell migration, and enhances growth factor-stimulated cell proliferation in culture (27, 28). As an adhesion substrate, CYR61 promotes cell spreading and adhesive signaling, resulting in the activation of focal adhesion kinase, paxillin, and Rac (9). CYR61 can regulate the expression of genes involved in angiogenesis and matrix remodeling, including vascular endothelial growth factor A (VEGF-A), VEGF-C, type I collagen, matrix metalloproteinase 1 (MMP1), and MMP3 (10). Furthermore, CYR61 induces neovascularization in corneal implants (3). These activities, as well as the expression of *Cyr61* in granulation tissue during wound healing, support a function for CYR61 in wound repair (10). Mechanistically, CYR61 functions as a ligand of multiple integrin receptors, including integrins $\alpha_v\beta_3$, $\alpha_v\beta_5$, $\alpha_6\beta_1$, $\alpha_{IIb}\beta_3$, and $\alpha_M\beta_2$, which mediate many of its activities in various cell types (11, 16, 24, 26, 42). Integrins and their ligands in the ECM have been implicated in angiogenesis and other morphogenetic events (22, 44). The specific roles of CYR61 in development, however, have remained unknown heretofore.

Abnormal angiogenesis contributes to the development and progression of a number of pathological conditions (15). Consistent with a role in angiogenesis, aberrant expression of *Cyr61* is associated with vascular diseases such as atherosclerosis,

* Corresponding author. Mailing address: Department of Molecular Genetics, University of Illinois at Chicago, 900 South Ashland Ave., Chicago, IL 60607-7170. Phone: (312) 996-6978. Fax: (312) 996-7034. E-mail: LFLau@uic.edu.

restenosis, and later-stage human breast cancer (10, 17, 41, 42, 47, 49). Furthermore, expression of *Cyr61* can promote tumor growth and vascularization (3, 49). Aside from their association with disease states, CYR61 and other CCN family members have been suggested to play an important role in embryonic development based on their expression in the fetal cardiovascular, skeletal, and nervous systems (Fig. 2J) (30, 32, 37). To determine the functions of CYR61 during development, we disrupted *Cyr61* in mice by gene targeting. We show here that *Cyr61* is an essential gene that plays novel roles in vascular development, regulating both vessel bifurcation in the placenta and large vessel integrity in the embryo. Phenotypes of *Cyr61* mutants bear intriguing similarities to those of mice lacking α_v integrins (4), which is consistent with the hypothesis that CYR61 may act as a physiological ligand of α_v integrins during development.

MATERIALS AND METHODS

Gene targeting. The *Cyr61* genomic DNA used in the targeting construct was cloned from a 129SvJ library (Stratagene). A *LacZ*-PGK-*neo* cassette was flanked by two *Cyr61* genomic DNA fragments, a 1.7-kb fragment including the promoter region at the 5′ end and a 3.7-kb fragment containing part of the coding region at the 3′ end. A PGK-*tk* cassette was positioned at the 5′ end of the promoter fragment with reversed transcription orientation. Transfection of the targeting construct DNA and the selection of the mutant embryonic stem (ES) cells (J1) were performed as described previously (33), except that the 2′-fluoro-2′-deoxy-1-β-D-arabinofuranosyl-5-iodouracil (FIAU) was replaced by 2 μM ganciclovir (a gift from Roche). Verification of the positive ES cell clones and genotyping of mice were carried out by Southern blot analysis and/or PCR by following standard procedures (20) (Fig. 1B and C). Two mutant ES cell clones, 2A11 and 4B7, were used to generate chimeric mice by blastocyst injection. Both clones yielded mutant mice with similar phenotypes, irrespective of their genetic background (C57BL/6J or 129SvJ). Most of the analysis was done on embryos derived from intercrosses with heterozygotes that were backcrossed with C57BL/6J at least twice. To verify that the targeted *Cyr61* allele is null, mouse embryonic fibroblasts were isolated from embryos on embryonic day 11.5 (E11.5 embryos), placed in culture, and stimulated with serum for 60 min. Total cell lysates were subjected to Western blot analysis with anti-CYR61 antiserum.

Histology, immunohistochemistry, and the terminal deoxynucleotidyltransferase-mediated dUTP-biotin nick end labeling (TUNEL) assay. Embryos were fixed in buffered 10% formalin and embedded in paraffin, and 7-μm-thick sections were prepared for standard hematoxylin and eosin staining. Yolk sacs were fixed in buffered formalin and stained with hematoxylin. For immunostaining, embryos were fixed in 4% paraformaldehyde; embedded in OCT; sectioned (7 μm); probed with monoclonal anti-platelet endothelial cell adhesion molecule 1 (anti-PECAM-1; Pharmingen), monoclonal anti-α-smooth-muscle actin (clone 1A4; Sigma), monoclonal anti-desmin (ZC18; Zymed), affinity-purified polyclonal anti-VEGF-A (sc-1836; Santa Cruz), and anti-VEGF-C (sc-9047; Santa Cruz) antibodies; and detected with either peroxidase (PECAM-1, VEGF-A, and VEGF-C) or alkaline phosphatase (α-smooth-muscle actin and desmin) chromogen. All histological and immunohistochemical analyses were carried out on embryos that were still alive at the time of harvest.

To detect the expression of *LacZ*, *Cyr61*$^{+/-}$embryos were processed and stained as described previously (20). TUNEL assays were done on cryopreserved sections (~7 μm thickness) with a fluorescein in situ cell death detection kit (Roche Molecular Biochemicals) by following the manufacturer's protocol.

RNA analysis. To study the effects of CYR61 on *Vegf-C* gene expression, mouse embryonic fibroblasts isolated from E14.5 wild-type (WT) CD-1 embryos were serum starved for 24 h and then treated with 10 μg of purified recombinant mouse CYR61/ml (27) in serum-free media for various times. Total cellular RNA was isolated, resolved on an agarose-formaldehyde gel, and blotted onto a nylon membrane by following standard protocols. Partial mouse *Vegf-C* cDNA was generated by reverse transcription-PCR with primers corresponding to nucleotides 202 to 222 and 757 to 779 (GenBank accession no. U73620). Human *GAPDH* cDNA was purchased from the American Type Culture Collection. Probes were radiolabeled by enzymatic incorporation of [^{32}P]dCTP. The blots were hybridized to the labeled probes and washed at high stringency (0.1× SSC [1× SSC is 0.15 M NaCl plus 0.015 M sodium citrate], 0.1% sodium dodecyl sulfate; 65°C), and the hybridization signal was quantified by the Phosphorimager (Molecular Dynamics) apparatus.

Transmission electron microscopy. Placentae were harvested and immersion fixed with 2.5% glutaraldehyde overnight at 4°C. Following fixation, the tissue was washed three times in phosphate-buffered saline and then postfixed in aqueous 1% OsO4–1% $K_3Fe(CN)_6$ for 1 h. Following three washes with phosphate-buffered saline, the tissue was dehydrated through a graded series of 30 to 100% ethanol–100% propylene oxide and then infiltrated in a 1:1 mixture of propylene oxide–Polybed 812 epoxy resin (Polysciences, Warrington, Pa.) for 1 h. After several changes of 100% resin over 24 h, pellets were embedded in molds and cured at 37°C overnight, followed by additional hardening at 65°C for two more days. Ultrathin (60-nm) cross sections of placenta were collected on copper grids and stained with 2% uranyl acetate in 50% methanol for 10 min, followed by staining with 1% lead citrate for 7 min. Sections were photographed by using a JEM 1210 transmission electron microscope (JEOL, Peabody, Ma.) at 80 kV onto electron microscope film (ESTAR thick base; Kodak, Rochester, N.Y.).

RESULTS

Disruption of murine *Cyr61* causes embryonic lethality. We disrupted *Cyr61* in mice by homologous recombination, replacing the translation start site and exon 1 through part of exon 2 with the *LacZ*-neomycin resistance cassette (Fig. 1A). The targeting construct was transfected into J1 ES cells, and recombinants were identified by Southern blot and PCR analyses (Fig. 1B and C, respectively). The resulting targeted allele expressed *lacZ* under the *Cyr61* promoter while shifting the remaining *Cyr61* coding sequence out of frame. Chimeric mice capable of germ line transmission were generated with two independently targeted ES cell clones, and the offspring of both yielded mutant mice with similar phenotypes. Heterozygous *Cyr61*$^{+/-}$mice expressed β-galactosidase in a manner that accurately recapitulates expression of the *Cyr61* gene, as judged by comparing β-galactosidase staining patterns with those from the localization of *Cyr61* mRNA and protein by in situ hybridization and immunohistochemistry (27, 30, 35, 48). To confirm that the targeted allele is null, embryo fibroblasts were isolated from *Cyr61*$^{-/-}$ embryos and their heterozygous and WT littermates. WT embryo fibroblasts expressed a robust amount of *Cyr61* mRNA upon serum stimulation; this was expected since *Cyr61* is an immediate-early gene inducible by serum growth factors (36). No *Cyr61* mRNA was detected in *Cyr61*$^{-/-}$ fibroblasts, even after serum stimulation (data not shown). Likewise, immunoblot analysis showed that CYR61 was completely absent from *Cyr61*$^{-/-}$ embryo fibroblasts, confirming that the targeted allele is indeed null (Fig. 1D). Consistent with gene dosage effects, the level of CYR61 in *Cyr61*$^{+/-}$fibroblasts was ~50% of that in *Cyr61*$^{+/+}$ fibroblasts.

Whereas *Cyr61* heterozygotes were viable and fertile, all *Cyr61*$^{-/-}$ mice died prenatally or perinatally and none survived beyond 24 h of birth (141 *Cyr61*$^{+/+}$ mice, 225 *Cyr61*$^{+/-}$mice, and 0 *Cyr61*$^{-/-}$ mice). To determine the onset of embryonic lethality, we isolated and genotyped fetuses at various stages of gestation. Intercrosses of heterozygotes yielded WT, heterozygous, and homozygous *Cyr61* mutants in Mendelian ratios at E9.5, although some *Cyr61*$^{-/-}$ embryos were already moribund (Table 1). About 30% of *Cyr61*$^{-/-}$ embryos had died by E10.5 due to a failure in chorioallantoic fusion, as the placenta supplants the yolk sac in providing the metabolic needs of the embryo (Table 1; Fig. 2A). The vascular structure of the yolk sac appeared normal in *Cyr61* mutants (Fig. 2G and H), indicating that vasculogenesis was not impaired in this tissue. Consistent with a direct role for *Cyr61* in chorioallantoic fusion, its

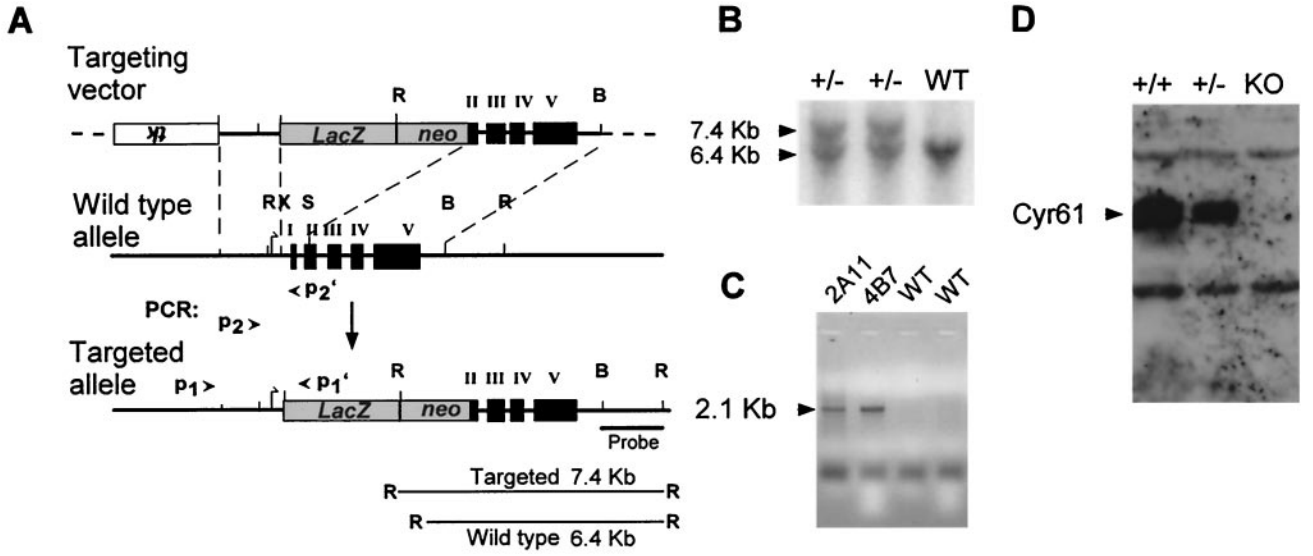

FIG. 1. Gene targeting of *Cyr61* in mice. (A) Targeting vector. The *Cyr61* genomic locus was disrupted by replacement of the *Xho*I-*Sma*I fragment, which includes the translation start site, exon I, and half of exon II, with a *LacZ*-PGK-*neo* cassette after homologous recombination. B, *Bam*HI; R, *Eco*RI; S, *Sma*I; X, *Xho*I. (B) Southern blot analysis. DNA isolated from ES cell clones was digested with *Eco*RI and probed with a *Bam*HI-*Eco*RI fragment (panel A), yielding 6.4- and 7.4-kb bands for the WT and targeted alleles, respectively. (C) PCR. Homologous recombination was confirmed by using a PCR primer pair, P1 and P1′ (panel A), to amplify a 2.1-kb fragment specific to the targeted allele. ES cell clones 2A11 and 4B7 showed the targeted allele. Additionally, PCR primer pairs (P2-P2′ and P2-P1′) yielded a 388-bp fragment and a 600-bp fragment from the WT and targeted alleles, respectively (data not shown). (D) Western blot analysis. Mouse embryo fibroblasts isolated from E11.5 embryos were stimulated with 10% serum for 1 h; total cell lysates were probed with anti-CYR61 antibodies after electrophoresis. KO, knockout.

expression was detected in both the allantois and the chorion in the E7.5 embryo just prior to the fusion event at E8.5 (Fig. 2I) (39). The majority of *Cyr61*$^{-/-}$ embryos exhibited successful chorioallantoic fusion and developed further but died at midgestation due to vascular defects. More than 70% of mutant embryos analyzed between E11.5 and E14.5 perished from hemorrhage and/or placental defects of varying degrees of severity (Table 1; Fig. 2C, E, and F). Only a few *Cyr61*$^{-/-}$ offspring resulting from multiple *Cyr61*$^{+/-}$intercrosses developed to term and were born alive, but these mice died within 1 day of birth. Investigation into the cause of this perinatal lethality has been hampered by the rarity of its occurrence.

Defective vessel bifurcation in the *Cyr61*$^{-/-}$ chorioallantoic junction. After chorioallantoic fusion, the allantoic artery and vein undergo extensive nonsprouting angiogenesis. The parental vessels elongate and bifurcate into smaller daughter vessels (Fig. 3E), which undergo further bifurcation to develop a network of vessels that covers the chorionic plate (Fig. 3A). Sprouting angiogenesis then emanates from this network to produce the finer embryonic vessels that interact with chorionic trophoblasts to form part of the labyrinth, where fetal-maternal exchange of gases, nutrients, and wastes occurs (Fig. 3I) (12, 39). In WT embryos, vessels undergoing bifurcation could be observed in the chorioallantoic junction (Fig. 3A and E). By contrast, vessel bifurcation was severely impaired in *Cyr61*$^{-/-}$ embryos and the few vessels present appeared compressed by the surrounding tissue (Fig. 3B and F). *Cyr61* expression was detected in the chorioallantoic junction at E9.5 (data not shown), and when the vascular structure was more defined by E10.5, *Cyr61* expression was clearly discerned in the allantoic mesoderm and endothelial linings of bifurcating vessels (Fig. 5A). Thus, *Cyr61* is expressed in the allantoic mesoderm, concordant with the initiation and progression of vessel bifurcation following chorioallantoic fusion.

TABLE 1. Genotypes of offspring derived from intercrosses of *Cyr61*$^{+/-}$ mice

Age	No. of litters	+/+	+/−	−/−[a]			R[b]
				N	P,H	D	
E9.5	8	14	32	10	3	0	0
E10.5	14	47	58	21	1	13	7
E11.5	21	36	53	8	9	9	4
E12.5	47	72	146	25	30	25	43
E13.5	39	89	119	14	15	40	44
E14.5	13	48	72	2	7	20	34

[a] N, morphologically normal embryos with no apparent phenotype; P,H, moribund embryos showing signs of placental defects and/or hemorrhage but with detectable heartbeat; D, deteriorated embryos with no heartbeat.
[b] R, resorbed embryos with a genotype that could not be determined.

Both WT and *Cyr61*$^{-/-}$ placentae developed into well-differentiated zones of similar thicknesses (Fig. 3C and D). In the WT labyrinth, networks of maternal blood sinuses interdigitated with fetal blood vessels, which were readily identified by the primitive nucleated embryonic red blood cells they carried (Fig. 3G). The *Cyr61*$^{-/-}$ labyrinth was dominated by saturated maternal blood sinuses, with few embryonic vessels visible (Fig. 3H). Immunostaining for PECAM-1 confirmed the paucity of embryonic vessels in the *Cyr61*$^{-/-}$ labyrinth (Fig. 4A and B). A higher-power view of PECAM-1-stained sections showed the presence of embryonic red blood cells in endothelial tubules, whereas the endothelial cells in the *Cyr61*$^{-/-}$ labyrinth were compressed and devoid of associated embryonic red blood

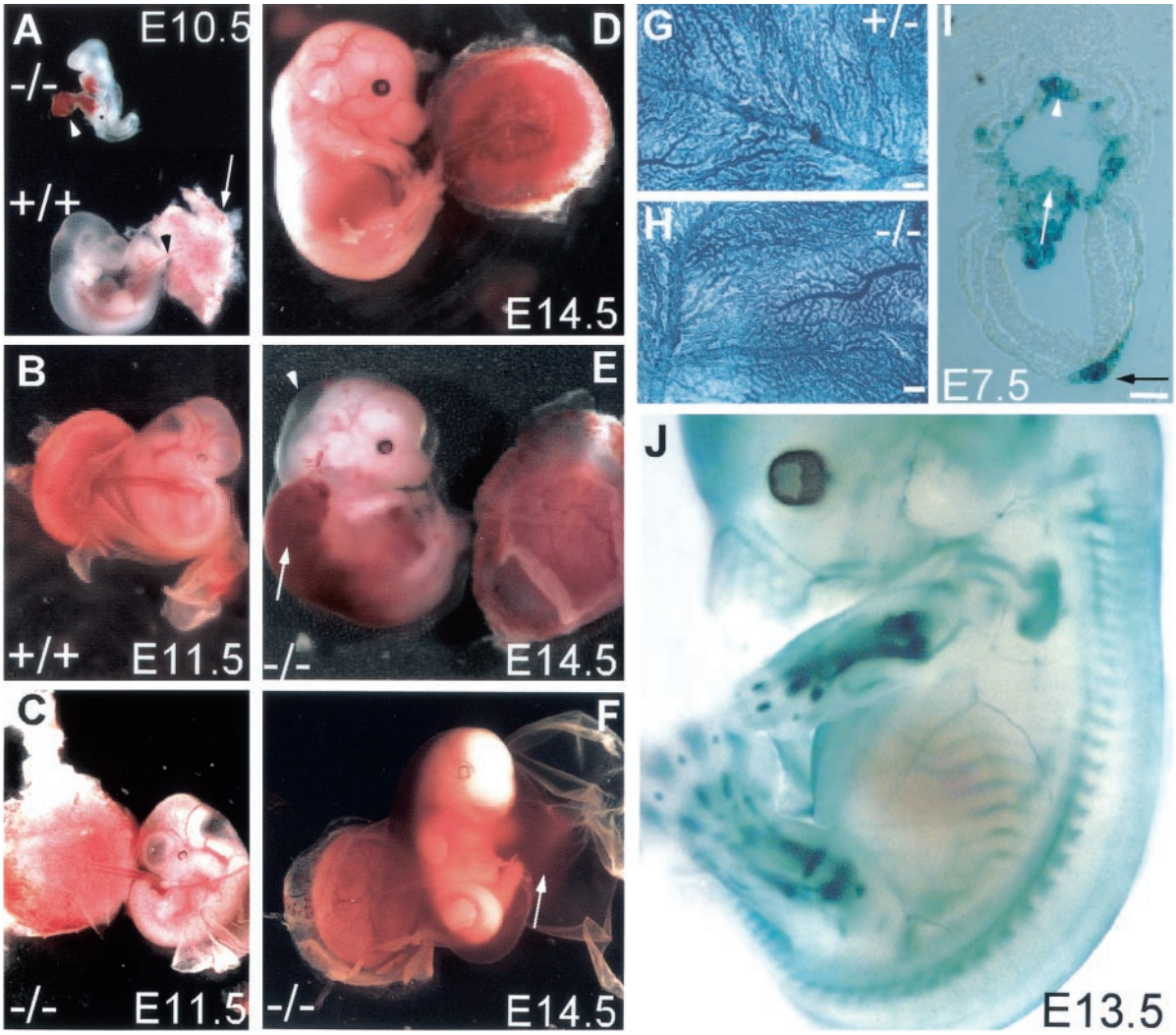

FIG. 2. Embryonic lethality in *Cyr61*-deficient mutants. (A) Chorioallantoic fusion occurred in WT embryos by E10.5, with the allantois (black arrowhead) attached to the placenta (white arrow). In some $Cyr61^{-/-}$ embryos, the allantois (white arrowhead) failed to fuse with the placenta, resulting in atrophy. (B) WT embryos at E11.5 showing successful chorioallantoic fusion and healthy placenta. (C) Some $Cyr61^{-/-}$ embryos at E11.5 showing successful chorioallantoic fusion but displaying vascular deficiency in the chorionic plate, resulting in a relatively pale placenta. (D) WT E14.5 embryo. (E) $Cyr61^{-/-}$ embryo (littermate of that shown in panel D) that developed to E14.5, exhibiting edema (arrowhead) and hemorrhage (arrow). (F) Other embryos obtained from E14.5 litters. These embryos were moribund, showing evidence of hemorrhage from the umbilical artery, filling the amnion. Vascular structure appeared normal in hematoxylin-stained yolk sacs from E10.5 $Cyr61^{+/-}$(G) and $Cyr61^{-/-}$ (H) embryos. Bars in panels G and H, 200 μm. (I) Expression of β-galactosidase driven by the *Cyr61* promoter. Expression was detected in both the chorion (white arrowhead) and the allantois (white arrow) at E7.5, when the allantois approached the chorion for eventual fusion. *LacZ* expression was also detected in the notochordal plate (black arrow). Bar, 10 μm. (J) Whole-mount staining of an E13.5 embryo showing *LacZ* expression in the sclerotomes of somites, endochondral bones (including those in fore- and hind limbs, digits, and ribs), and large arteries.

cells (Fig. 4C and D). However, CYR61 is unlikely to play a direct role in the labyrinth inasmuch as *Cyr61* is expressed in trophoblast giant cells (Fig. 5C) but not in labyrinth trophoblasts (Fig. 5B) (35) and CYR61 acts locally due to its high-affinity binding to the ECM upon secretion (51). Moreover, high levels of VEGF-A were detected in both the WT and $Cyr61^{-/-}$ labyrinth by immunostaining (Fig. 4E and F) (13), thereby assuring the presence of a potent inducer for sprouting angiogenesis in the labyrinth. These results indicate that, although $Cyr61^{-/-}$ placentae exhibited severe deficiency in labyrinthine embryonic vasculature, such defects originates at the chorioallantoic junction, where nonsprouting angiogenesis failed.

These results show that CYR61 plays a novel role in regulating vessel bifurcation, and to our knowledge, analysis of $Cyr61^{-/-}$ mice provides the first description of a specific genetic defect in vessel bifurcation in any tissue. In an effort to understand how CYR61 might act, we examined the expression of genes known to affect vessel development. The expression of *Vegf-A*, *Ang-1*, *Ang-2*, and *Tie-2* (50) was unaltered by CYR61 deficiency (data not shown). However, whereas VEGF-C was detected in the WT allantoic mesoderm at E9.5, coincident with *Cyr61* expression (Fig. 5A; data not shown), it was undetectable in $Cyr61^{-/-}$ embryos (Fig. 5D and E). These results suggest that CYR61 might act in part through the upregulation of specialized angiogenic factors such as VEGF-C,

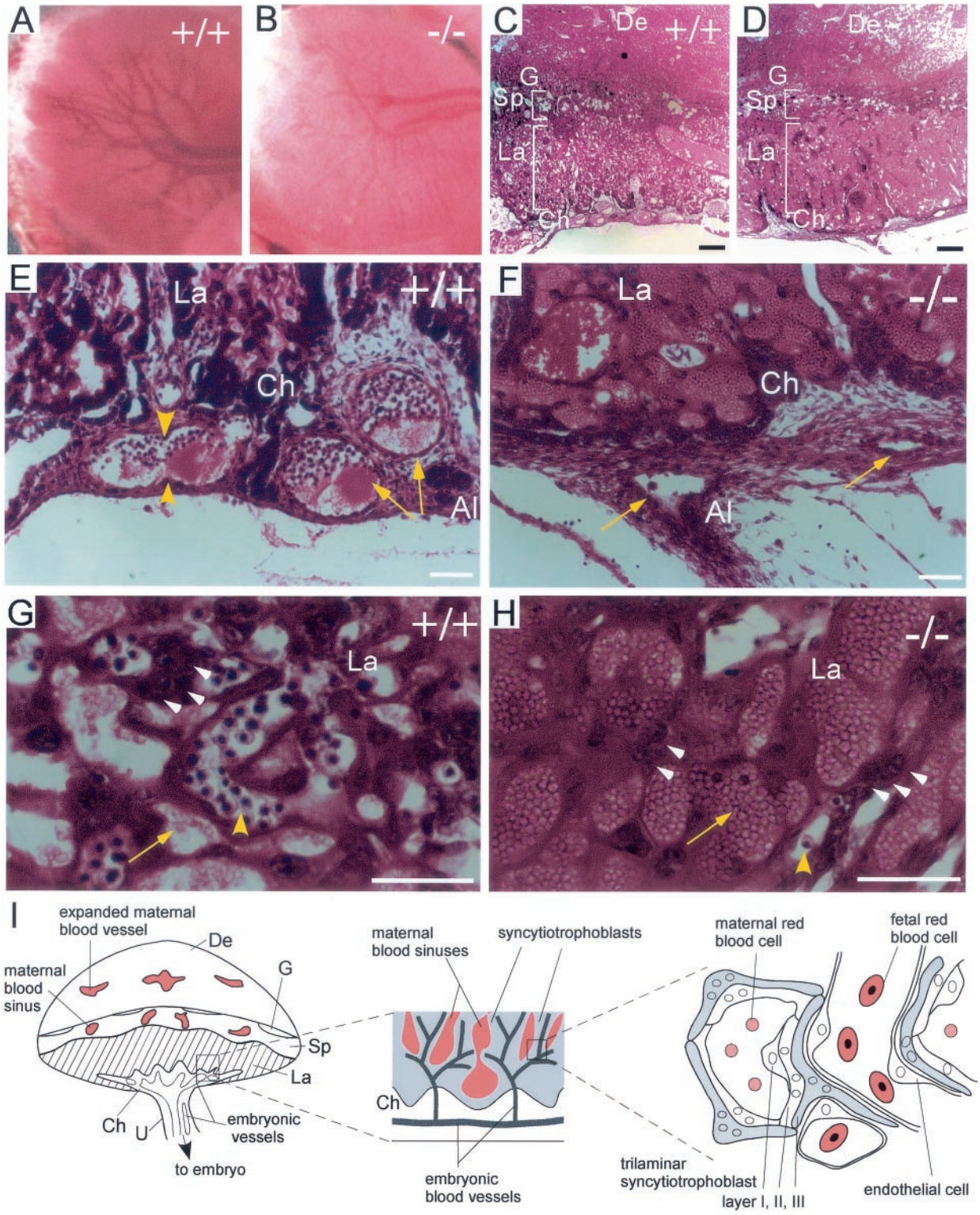

FIG. 3. Histological analysis of placental defects in *Cyr61*$^{-/-}$ embryos. At E12.5, vessel branches had developed in the chorionic plate of the WT (A) but not *Cyr61*$^{-/-}$ (B) placenta. Hematoxylin and eosin staining revealed that both WT (C) and null (D) placentae developed differentiated zones, including the chorionic plate (Ch), the labyrinth (La), and the spongiotrophoblast layer (Sp) adjacent to the maternal decidua (De). Close-up view (E) shows vessels (arrowheads) undergoing or having completed (arrows) nonsprouting angiogenesis, thus bifurcating the parental vessels at the WT chorionic plate. Al, allantois; G, giant cells. Vessels (arrows) in the *Cyr61*$^{-/-}$ chorionic plate appear compressed, and no bifurcation was observed (F). Unlike the WT labyrinth (G), where fetal vessels containing nucleated red blood cells (yellow arrowhead) interdigitate with maternal blood sinuses (yellow arrow), the *Cyr61*$^{-/-}$ labyrinth (H) was predominantly saturated with maternal blood sinuses (arrow) and few fetal vessels were found. Trophoblast nuclei (white arrowheads) were evident in both WT and mutant labyrinth (G and H). A schematic representation of the mouse placenta, with expanded views of the labyrinthine zone, is also shown (I). U, umbilical cord. White bars, 50 μm; black bars in panels C and D, 200 μm.

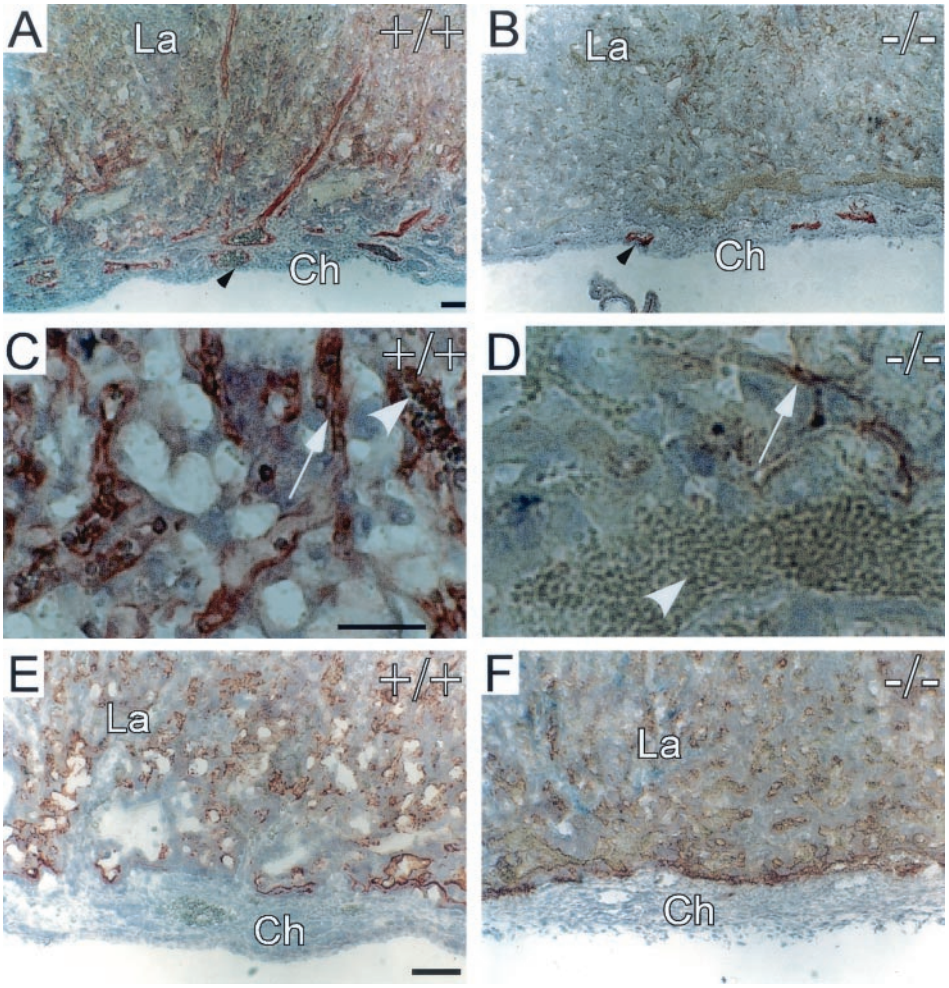

FIG. 4. Immunostaining of *Cyr61*$^{-/-}$ placenta. (A) PECAM-1 staining for endothelial cells showed the embryonic vessels (arrowhead) in the WT chorionic plate and labyrinth. (B) Drastically fewer PECAM-staining endothelial cells (arrowhead) were found in the *Cyr61*$^{-/-}$ placenta. (C) Higher magnification views show that the PECAM-staining fetal vessels (arrow) contained embryonic red blood cells (arrowhead) in the WT labyrinth. (D) In contrast, endothelial cells (arrow) of the *Cyr61*$^{-/-}$ labyrinth appeared compressed and carried no apparent red blood cells. The white arrowhead in panel D points to maternal blood cells. Despite deficient vascularization of the *Cyr61*$^{-/-}$ labyrinth, no difference in VEGF-A expression between the WT (E) and *Cyr61*$^{-/-}$ (F) placentae could be detected by immunostaining. Similar expression of Tie-2 was also observed in WT and *Cyr61*$^{-/-}$ placentae (data not shown). Ch, chorion, La, labyrinth. Bars, 50 μm.

known to induce both angiogenesis and lymphangiogenesis (8). To assess the ability of CYR61 to regulate *Vegf-C* expression, we evaluated *Vegf-C* mRNA levels in response to purified recombinant CYR61 protein in mouse embryonic fibroblasts isolated from WT E14.5 embryos. Indeed, CYR61 treatment upregulated *Vegf-C* mRNA levels, with a notable response within 2 h after CYR61 addition (Fig. 5F). Upregulation of *Vegf-C* mRNA occurred sixfold by 6 h, and a high level of mRNA was sustained for least 24 h after CYR61 treatment. Consistent with this observation, purified CYR61 has been shown to upregulate *Vegf-C* mRNA and protein in human fibroblasts (10).

Differentiation of labyrinth trophoblasts in *Cyr61*$^{-/-}$ placenta. Separating the maternal blood sinuses and fetal vessels in the placental labyrinth are differentiated trophoblasts that form a trilaminar barrier, which is comprised of two layers of syncytiotrophoblasts and a mononuclear trophoblast layer (Fig. 3I and 6A) (19). Upon contact of the allantois with the chorion, trophoblasts at the chorionic plate begin to fold, invaginate, and undergo extensive villous branching together with their associated fetal blood vessels (39). These chorionic trophoblasts differentiate and undergo cell fusion, giving rise to a syncytiotrophoblast layer that is directly juxtaposed to the endothelial cells of fetal blood vessels. Adjacent to this syncytium is a second layer of syncytiotrophoblasts derived from ectoplacental trophoblast cells. Lying outside of the two syncytiotrophoblast layers and in direct contact with maternal blood is a layer of mononuclear trophoblasts (Fig. 3I).

The *Cyr61*$^{-/-}$ placental labyrinth appeared highly structured despite the dearth of embryonic vessels (Fig. 3D). The maternal blood sinuses were well delineated, suggesting the presence of differentiated trophoblasts that separate them (Fig. 3H). Under transmission electron microscopy, the trilaminar trophoblast barrier was readily observed in the WT labyrinth (Fig. 6A). Interestingly, although few embryonic vessels were found in the *Cyr61*$^{-/-}$ labyrinth, where they did occur, they were

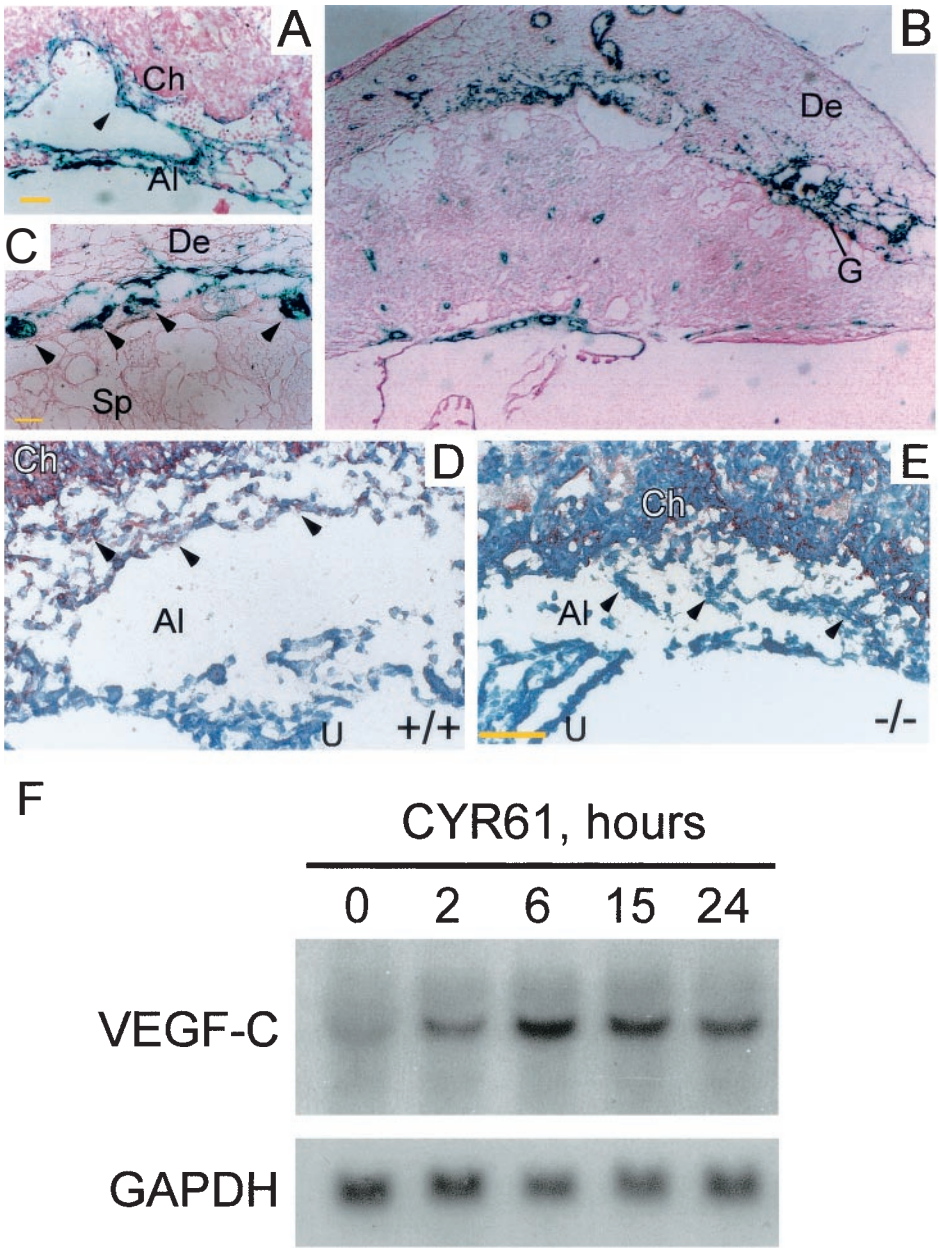

FIG. 5. (A) β-Galactosidase staining was detected at the chorioallantoic junction at E10.5, when embryonic vessels were actively bifurcating and invaded the placenta. Intense staining was found in the allantoic mesoderm and inner endothelial lining associated with bifurcating vessels (arrowhead). (B) By E13.5, β-galactosidase staining was localized to the vessels in the chorionic plate, maternal decidua, and trophoblast giant cells. (C) Higher magnification of panel B is given to demonstrate staining in giant cells (arrowheads). (D) VEGF-C was detected in the allantoic mesoderm (arrowheads) and chorion of WT E9.5 placenta by immunostaining but not in allantoic mesoderm of *Cyr61*$^{-/-}$ placenta (E). (F) In Northern blot analysis, serum-starved mouse embryonic fibroblasts isolated from E14.5 WT embryos were treated with purified recombinant CYR61 for various durations before the total RNA was isolated. *Vegf-C* mRNA was upregulated sixfold after 6 h of CYR61 treatment, and this upregulation was sustained for at least 24 h. The hybridization signal was quantified by Phosphorimager. Al, allantois; Ch, chorion; De, decidua; G, giant cells; La, labyrinth; Sp, spongiotrophoblast; U, umbilical cord. Yellow bars, 50 μm.

encased by an organized and normally structured trilaminar trophoblast barrier (Fig. 6B). The *Cyr61*$^{-/-}$ labyrinth also presented a unique feature normally not found in WT labyrinth: pools of maternal blood sinuses devoid of fetal vessels (Fig. 3H). The trilaminar structure was absent among these maternal blood sinuses, as no barrier was needed. Instead, separating the maternal blood sinuses were syncytiotrophoblasts derived from ectoplacental trophoblasts (Fig. 6C), judging from their large nuclei and lack of lipid vesicles (19). These data show that the invasion of chorionic trophoblasts into the labyrinth and their differentiation were not impaired in *Cyr61* mutants and that formation of the trilaminar trophoblast barrier was unaffected. Furthermore, differentiation and syncytial cell fusion of ectoplacental trophoblasts can occur in the absence of

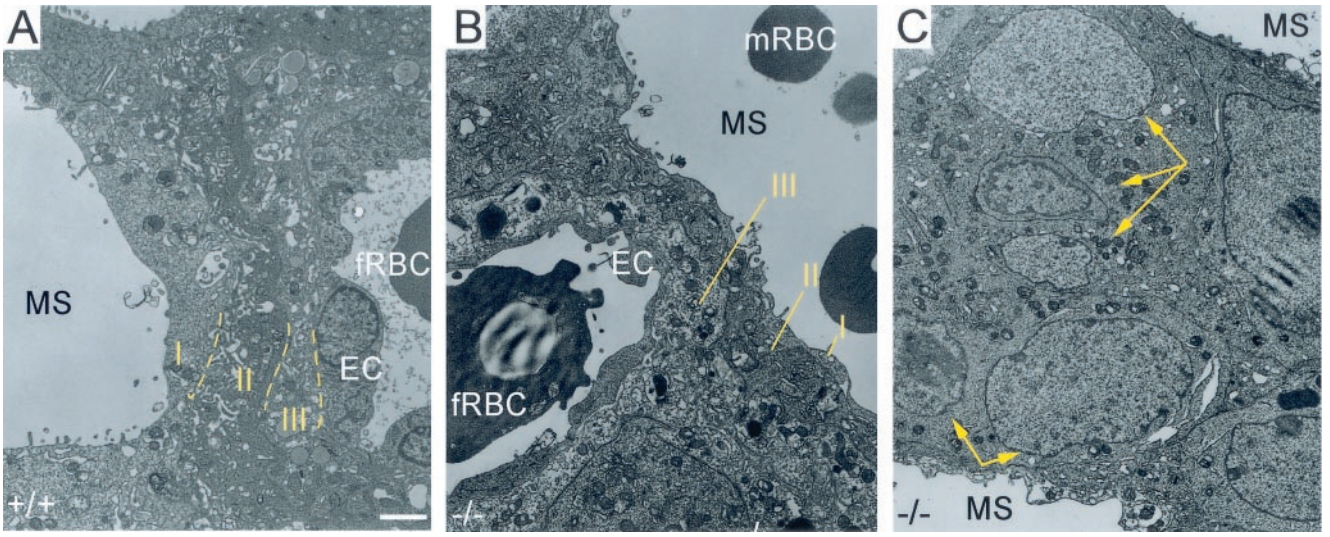

FIG. 6. Transmission electron micrographs of the E12.5 labyrinth. Both WT (A) and *Cyr61*$^{-/-}$ (B) labyrinths displayed the trilaminar barrier composed of two layers of syncytiotrophoblasts (II and III) in addition to a layer of mononuclear trophoblasts (I). In the *Cyr61*$^{-/-}$ labyrinth, where maternal blood sinuses dominate (C), ectoplacental trophoblasts differentiated and formed syncytium (yellow arrows point to multiple nuclei within fused cells) without neighboring embryonic vessels. EC, endothelial cells; fRBC, fetal red blood cells; mRBC, maternal red blood cells; MS, maternal blood sinuses. White bar, 2 μm.

juxtaposed chorionic trophoblasts or neighboring embryonic vasculature.

Compromised large-vessel integrity in *Cyr61*$^{-/-}$ embryos. Vascular defects in *Cyr61* mutants were not confined to the placenta. The large vessels in *Cyr61*$^{-/-}$ embryos were unstable and leaky, resulting in severe hemorrhage and edema (Fig. 2E). Such defects were frequently found in the dorsal aorta and umbilical arteries. A direct role for CYR61 in vessel integrity is consistent with the high levels of *Cyr61* expression in the endothelial linings of large arteries during early vascular development; this expression was expanded to the vessel wall after the recruitment of smooth-muscle cells (Fig. 7K). The level of *Cyr61* expression was dramatically higher in arteries than in veins, and consistently, most of the hemorrhaging occurred in *Cyr61*$^{-/-}$ arteries.

Transverse sections of the *Cyr61*$^{-/-}$ dorsal aorta revealed a severely disorganized vascular structure, with vascular cells being loosely associated with or detached from a disintegrated basal lamina (Fig. 7B). Remarkably, the *Cyr61*$^{-/-}$ dorsal aorta was enormously dilated, resembling a large aneurysm (compare Fig. 7C and E to 7D and F). Immunostaining showed that PECAM-positive endothelial cells were not consistently found in the inner lining of the aorta, and in some areas, endothelial cells were found in the surrounding tissue (arrow in Fig. 7D). Deficits in vascular smooth-muscle cells (VSMCs) and pericytes that normally surround the vessel wall were also observed, since only parts of the dilated vessels stained positive for desmin, a marker for pericytes (Fig. 7G and H), or α-smooth-muscle actin, a marker for VSMCs (Fig. 7E and F). Despite these deficits, the presence of both pericytes and VSMCs suggests that the recruitment of pericytes and VSMCs was able to proceed in *Cyr61*$^{-/-}$ mice. The deficits in pericytes and VSMCs may be a consequence of vessel dilation, and thereby, many more cells would be required to fully surround the lumen. Based on the known activities of CYR61, it appears likely that CYR61 deficiency may have impaired vessel integrity by having detrimental effects on the interactions among VSMCs, the endothelial lining, and their surrounding ECM.

An essential role for CYR61 in the maintenance of vessel integrity is further supported by the observation that some of the vascular cells in *Cyr61*$^{-/-}$ embryos appeared to be undergoing apoptosis (Fig. 7B). Indeed, TUNEL analysis confirmed that many vascular cells were apoptotic (Fig. 7I and J). Interestingly, expression of *Ang-1* and its receptor *Tie-2*, which are important for pericyte recruitment and vascular integrity (34, 46), was not disrupted in *Cyr61*$^{-/-}$ embryos (data not shown). These results demonstrate a critical and unique role for CYR61 in supporting vascular integrity and vascular cell survival in major arteries after the vessels are formed.

DISCUSSION

Although CYR61 has been shown to induce angiogenesis, its functions during development were previously unknown. In this study, we demonstrated by targeted gene disruption that *Cyr61* is an essential gene for mammalian vascular development. Whereas ~30% of *Cyr61*-null mice die from defects in chorioallantoic fusion, the majority (~70%) perish from vascular defects that include impaired allantoic vessel bifurcation in the placenta and compromised vascular integrity in embryonic arteries. Furthermore, many of the phenotypes observed in *Cyr61*-null mice are consistent with known activities of purified CYR61 protein, which functions largely through integrin-mediated mechanisms (16, 31).

Several phenotypes of *Cyr61*-null mice are unexpected. Although *Cyr61* is prominently expressed in trophoblast giant cells and in the ectoplacental cone (35), the normal Mendelian ratio of *Cyr61* mutant embryos at E9.5 suggests that CYR61 is not critical for implantation. In addition, *Cyr61* is not required for vasculogenesis, since formation of the major embryonic

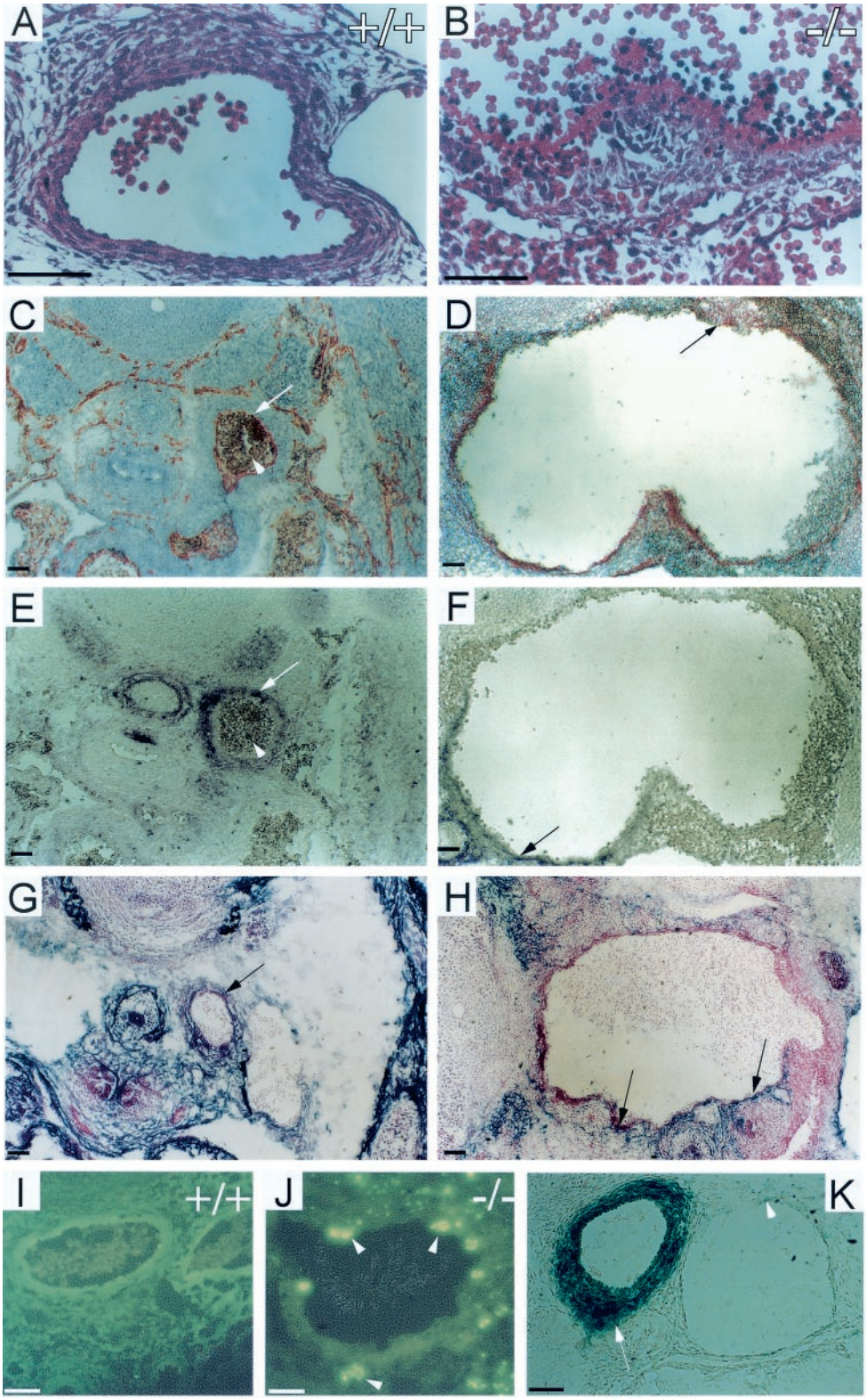

FIG. 7. Hemorrhage of the dorsal aorta in *Cyr61*-deficient E13.5 embryos. (A, C, E, G, I) WT embryos. (B, D, F, H, J) *Cyr61*$^{-/-}$ embryos. Hematoxylin and eosin staining showed completely disorganized vascular cells (B) in the *Cyr61*$^{-/-}$ dorsal aorta compared to that for the WT (A). Transverse sections were immunostained for PECAM-1 (C and D), α-smooth-muscle actin (E and F), and desmin (G and H), showing the drastically dilated lumen in *Cyr61*$^{-/-}$ embryos. The endothelial lining (arrows in panels C and D), the smooth-muscle cell wall (arrows in panels E and F), and the pericytes (arrows in panels G and H) of the aorta were disorganized compared to that for the WT, with the apparent mixing of endothelial cells, VSMCs, and pericytes. WT (I) and *Cyr61*$^{-/-}$ (J) dorsal aorta sections were subjected to TUNEL analysis; apoptotic cells are identified by green fluorescence (arrowheads). β-Galactosidase staining was prominent in arteries such as the dorsal aorta (arrow) but nearly undetectable in the vein (arrowhead) (K). Bars, 50 μm.

vessels and the primary vascular plexus of the yolk sac is successful in *Cyr61* mutants. However, about 30% of *Cyr61*-null embryos failed to establish chorioallantoic fusion and succumbed by E10.5. CYR61 is known to support cell adhesion and regulate matrix protein synthesis and degradation (9, 10) and may therefore mediate cell-cell adhesion in chorioallantoic fusion and/or establish a matrix environment in which fusion can occur. Attachment of the allantois to the chorion likely involves multiple cell adhesion molecules, including α_4 integrins and vascular cell adhesion molecule 1 (VCAM-1) (18, 29, 52). As in the case of *Cyr61* mutants, chorioallantoic attachment defects exhibited in mutants deficient in α_4 integrins or VCAM-1 are also incompletely penetrant. Thus, in addition to cell adhesion molecules such as α_4 integrins and VCAM-1, CYR61 may play a role as a cell adhesive protein to participate in chorioallantoic attachment.

CYR61 deficiency results in a specific defect in vessel bifurcation at the chorioallantoic junction, leading to severe undervascularization in the placental labyrinth. To our knowledge, analysis of *Cyr61*-null mutants affords the first description of a specific genetic defect in vessel bifurcation in any tissue and provides new insight into the players that regulate this aspect of vascular development. This novel phenotype is correlated with the impaired expression of *Vegf-C* in the allantoic mesoderm, suggesting that CYR61 may regulate vessel bifurcation either directly or indirectly through VEGF-C (Fig. 5D and E). Consistent with this observation, CYR61 is able to upregulate *Vegf-C* expression in mouse embryonic fibroblasts (Fig. 5F) and in cultured human fibroblasts (10). While VEGF-C is involved in both lymphangiogenesis and angiogenesis, it induces more vessel branching and less sprouting compared to VEGF-A (8), suggesting a role in vessel bifurcation. Although phenotypes of *Vegf-C*-null mice have not been described, those of mutants deficient in one of its receptors, VEGFR3, are consistent with a role for VEGF-C in the development of the cardiovascular system and in vessel morphogenesis (14).

The labyrinthine defect of *Cyr61*-null mice is distinct from those caused by disruptions of other genes, many of which affect trophoblasts (39). For example, deficiency for *Gcm-1* results in a labyrinthine malformation due to the defective branching morphogenesis of chorionic trophoblasts but allantoic nonsprouting angiogenesis is not affected (1, 43). By contrast, trophoblast differentiation and syncytiotrophoblast formation proceed normally in the *Cyr61*-null placenta, forming the trilaminar trophoblast barrier where fetal vessels are found. Therefore, the labyrinthine vascular deficiency in *Cyr61* mutants is not due to trophoblast defects. Interestingly, syncytiotrophoblasts of ectoplacental origin, rather than of the trilaminar structure, separate pools of maternal blood where no barrier from fetal vessels is needed. Inasmuch as pools of maternal blood sinuses devoid of fetal vessels are not normally observed in the WT labyrinth, these findings in the *Cyr61*-null placenta demonstrate that differentiation of ectoplacental trophoblasts occurs in the absence of cell-cell communication with juxtaposed chorionic trophoblasts or neighboring embryonic vasculature.

CYR61 is a ligand of, and binds directly to, integrins $\alpha_v\beta_3$ and $\alpha_v\beta_5$ and promotes cell adhesion and migration through these integrins (3, 16, 26). Thus, it may be informative to compare the phenotypes of *Cyr61*- and α_v integrin-null mice. However, many ligands are known to bind the five α_v integrins ($\alpha_v\beta_1$, $\alpha_v\beta_3$, $\alpha_v\beta_5$, $\alpha_v\beta_6$, and $\alpha_v\beta_8$) and CYR61 is also known to bind several other integrins ($\alpha_6\beta_1$, $\alpha_{IIb}\beta_3$, and $\alpha_M\beta_2$). Therefore, the phenotypes of α_v- and *Cyr61*-null mice are expected to be complex, reflecting the superimposed consequences of multiple ablated-receptor-ligand interactions. It is thus remarkable that there are intriguing similarities between *Cyr61* mutants and α_v integrin-deficient mice, which also suffer placental insufficiency and embryonic hemorrhage (4). About 80% of mice lacking all α_v integrins die by E11.5 due to undervascularization of the placental labyrinth, while the remaining 20% succumb perinatally with prominent intracerebral hemorrhages. Strikingly, the placental labyrinthine zone of α_v-null mice appears to be morphologically similar to that of the *Cyr61* mutant and fetal vessels at the chorionic plate also appear deficient and collapsed (4). While the binding of CYR61 to integrins $\alpha_v\beta_3$ and $\alpha_v\beta_5$ as a ligand has been established biochemically, these similarities in the phenotypes of *Cyr61*- and α_v-null mice are consistent with the hypothesis that CYR61 interacts with α_v integrins physiologically during development.

Cyr61-null embryos suffer from compromised large-vessel integrity. This defect suggests that CYR61 is involved in the maintenance of vessel integrity by stabilizing interactions among endothelial cells, VSMCs, and the ECM. Consistent with this interpretation, CYR61 has been shown to regulate the expression of various ECM molecules (10), support cell adhesion, and induce chemotaxis through integrin $\alpha_v\beta_3$ in endothelial cells and through integrin $\alpha_6\beta_1$ in VSMCs (3, 17, 26). Thus, the cell adhesive and chemotactic activities of CYR61 on endothelial and smooth-muscle cells may underlie the loss of vessel integrity in *Cyr61*$^{-/-}$ embryos. Furthermore, vascular cells in *Cyr61* mutants are prone to apoptotic death, consistent with the ability of CYR61 to support endothelial cell survival in culture (2, 32a). In this context, it is interesting to note that WISP-1, a CCN protein closely related to CYR61, can inhibit p53-mediated apoptosis through the activation of Akt (45).

Members of the CCN family of vertebrate-specific proteins may play overlapping but nonredundant roles during embryonic development. Given that CYR61 and CTGF exhibit remarkably similar activities in vitro and expression patterns in vivo (9, 32), it is surprising that their loss-of-function mutants display distinct phenotypes. *Ctgf*-deficient mice display generalized chondrodysplasia, leading to perinatal death due to respiratory failure (S. Ivkovic, S. N. Popoff, F. F. Safadi, M. Zhao, R. C. Stephenson, B. S. Yoon, A. Daluiski, P. Segarini, and K. M. Lyons, submitted for publication). Although *Cyr61* mutants did not reveal defects in skeletal development due to their early-embryonic lethality, expression of *Cyr61* is tightly associated with chondrogenesis during development and shows a pattern similar to that of *Ctgf* (Fig. 2J) (27, 35). Furthermore, purified CYR61 has been shown to promote chondrogenic differentiation in mouse limb bud mesenchymal cells (48). Loss of another CCN protein, WISP-3 (CCN6), causes progressive pseudorheumatoid dysplasia in humans (21), resulting in juvenile-onset cartilage degeneration. Thus, members of the CCN family may be important for different aspects or stages of cartilage development and maintenance. Likewise, although *Ctgf* mutants did not exhibit defects in vessel integrity or placental vasculature, they displayed angiogenic deficiency in the

growth plates during endochondral bone formation (S. Ivkovic et al., submitted). CTGF is therefore important for angiogenesis specific to skeletal development. Together, these findings establish that both CYR61 and CTGF are essential regulators for vertebrate embryogenesis and indicate that CCN proteins may serve tissue- and/or stage-specific functions in the development of the vascular and skeletal systems. Further investigation by conditional knockout strategies will help elucidate the tissue-specific functions of these CCN proteins.

ACKNOWLEDGMENTS

We are grateful to Hiroaki Kiyokawa for invaluable advice; Philippe Soriano and Rudolf Jaenisch for gifts of reagents; Shr-Jeng Leu for protein analysis; and Ana Bursick, Mara Sullivan, and Fengli Guo for technical assistance. We also thank Karen Lyons for sharing unpublished data and Jay Cross, Dan Linzer, Karen Lyons, and our colleagues for illuminating discussions.

This work was supported by grants from the NIH (CA46565 to L.F.L. and CA76541 to D.B.S.).

REFERENCES

1. **Anson-Cartwright, L., K. Dawson, D. Holmyard, S. J. Fisher, R. A. Lazzarini, and J. C. Cross.** 2000. The glial cells missing-1 protein is essential for branching morphogenesis in the chorioallantoic placenta. Nat. Genet. **25:** 311–314.
2. **Babic, A. M., C.-C. Chen, and L. F. Lau.** 1999. Fisp12/mouse connective tissue growth factor mediates endothelial cell adhesion and migration through integrin αVβ3, promotes endothelial cell survival, and induces angiogenesis in vivo. Mol. Cell. Biol. **19:**2958–2966.
3. **Babic, A. M., M. L. Kireeva, T. V. Kolesnikova, and L. F. Lau.** 1998. CYR61, product of a growth factor-inducible immediate-early gene, promotes angiogenesis and tumor growth. Proc. Natl. Acad. Sci. USA **95:**6355–6360.
4. **Bader, B. L., H. Rayburn, D. Crowley, and R. O. Hynes.** 1998. Extensive vasculogenesis, angiogenesis, and organogenesis precede lethality in mice lacking all alpha v integrins. Cell **95:**507–519.
5. **Bork, P.** 1993. The modular architecture of a new family of growth regulators related to connective tissue growth factor. FEBS Lett. **327:**125–130.
6. **Bornstein, P.** 1995. Diversity of function is inherent in matricellular proteins: an appraisal of thrombospondin 1. J. Cell Biol. **130:**503–506.
7. **Brigstock, D. R.** 1999. The connective tissue growth factor/cysteine-rich 61/nephroblastoma overexpressed (CCN) family. Endocr. Rev. **20:**189–206.
8. **Cao, Y., P. Linden, J. Farnebo, R. Cao, A. Eriksson, V. Kumar, J. H. Qi, L. Claesson-Welsh, and K. Alitalo.** 1998. Vascular endothelial growth factor C induces angiogenesis in vivo. Proc. Natl. Acad. Sci. USA **95:**14389–14394.
9. **Chen, C.-C., N. Chen, and L. F. Lau.** 2001. The angiogenic factors Cyr61 and CTGF induce adhesive signaling in primary human skin fibroblasts. J. Biol. Chem. **276:**10443–10452.
10. **Chen, C.-C., F.-E. Mo, and L. F. Lau.** 2001. The angiogenic inducer Cyr61 induces a genetic program for wound healing in human skin fibroblasts. J. Biol. Chem. **276:**47329–47337.
11. **Chen, N., C. C. Chen, and L. F. Lau.** 2000. Adhesion of human skin fibroblasts to Cyr61 is mediated through integrin α6β1 and cell surface heparan sulfate proteoglycans. J. Biol. Chem. **275:**24953–24961.
12. **Cross, J. C., Z. Werb, and S. J. Fisher.** 1994. Implantation and the placenta: key pieces of the development puzzle. Science **266:**1508–1518.
13. **Dumont, D. J., G. H. Fong, M. C. Puri, G. Gradwohl, K. Alitalo, and M. L. Breitman.** 1995. Vascularization of the mouse embryo: a study of flk-1, tek, tie, and vascular endothelial growth factor expression during development. Dev. Dyn. **203:**80–92.
14. **Dumont, D. J., L. Jussila, J. Taipale, A. Lymboussaki, T. Mustonen, K. Pajusola, M. Breitman, and K. Alitalo.** 1998. Cardiovascular failure in mouse embryos deficient in VEGF receptor-3. Science **282:**946–949.
15. **Folkman, J.** 2001. Angiogenesis-dependent diseases. Semin. Oncol. **28:**536–542.
16. **Grzeszkiewicz, T. M., D. J. Kirschling, N. Chen, and L. F. Lau.** 2001. CYR61 stimulates human skin fibroblast migration through integrin $\alpha_V\beta5$ and enhances mitogenesis through integrin $\alpha_V\beta3$, independent of its carboxyl-terminal domain. J. Biol. Chem. **276:**21943–21950.
17. **Grzeszkiewicz, T. M., V. Lindner, N. Chen, S. C. T. Lam, and L. F. Lau.** 2002. The angiogenic factor CYR61 supports vascular smooth muscle cell adhesion and stimulates chemotaxis through integrin α6β1 and cell surface heparan sulfate proteoglycans. Endocrinology **143:**1441–1450.
18. **Gurtner, G. C., V. Davis, H. Li, M. J. McCoy, A. Sharpe, and M. I. Cybulsky.** 1995. Targeted disruption of the murine VCAM1 gene: essential role of VCAM-1 in chorioallantoic fusion and placentation. Genes Dev. **9:**1–14.
19. **Hernandez-Verdun, D.** 1974. Morphogenesis of the syncytium in the mouse placenta. Ultrastructural study. Cell Tissue Res. **148:**381–396.
20. **Hogan, B., R. Beddington, F. Costantini, and E. Lacy.** 1994. Manipulating the mouse embyro. Cold Spring Harbor Press, Plainview, N.Y.
21. **Hurvitz, J. R., W. M. Suwairi, H. W. Van, H. El-Shanti, A. Superti-Furga, J. Roudier, D. Holderbaum, R. M. Pauli, J. K. Herd, H. E. Van, H. Rezai-Delui, E. Legius, M. M. Le, J. Al-Alami, S. A. Bahabri, and M. L. Warman.** 1999. Mutations in the CCN gene family member WISP3 cause progressive pseudorheumatoid dysplasia. Nat. Genet. **23:**94–98.
22. **Hynes, R. O.** 1996. Targeted mutations in cell adhesion genes: what have we learned from them? Dev. Biol. **180:**402–412.
23. **Imai, Y., A. Moralez, U. Andag, J. B. Clarke, W. H. Busby, Jr., and D. R. Clemmons.** 2000. Substitutions for hydrophobic amino acids in the N-terminal domains of IGFBP-3 and -5 markedly reduce IGF-I binding and alter their biologic actions. J. Biol. Chem. **275:**18188–18194.
24. **Jedsadayanmata, A., C. C. Chen, M. L. Kireeva, L. F. Lau, and S. C. Lam.** 1999. Activation-dependent adhesion of human platelets to Cyr61 and Fisp12/mouse connective tissue growth factor is mediated through integrin αIIbβ3. J. Biol. Chem. **274:**24321–24327.
25. **Kalus, W., M. Zweckstetter, C. Renner, Y. Sanchez, J. Georgescu, M. Grol, D. Demuth, R. Schumacher, C. Dony, K. Lang, and T. A. Holak.** 1998. Structure of the IGF-binding domain of the insulin-like growth factor-binding protein-5 (IGFBP-5): implications for IGF and IGF-I receptor interactions. EMBO J. **17:**6558–6572.
26. **Kireeva, M. L., S. C. T. Lam, and L. F. Lau.** 1998. Adhesion of human umbilical vein endothelial cells to the immediate-early gene product Cyr61 is mediated through integrin αVβ3. J. Biol. Chem. **273:**3090–3096.
27. **Kireeva, M. L., B. V. Latinkic, T. V. Kolesnikova, C.-C. Chen, G. P. Yang, A. S. Abler, and L. F. Lau.** 1997. Cyr61and Fisp12 are both signaling cell adhesion molecules: comparison of activities, metabolism, and localization during development. Exp. Cell Res. **233:**63–77.
28. **Kireeva, M. L., F.-E. Mo, G. P. Yang, and L. F. Lau.** 1996. Cyr61, product of a growth factor-inducible immediate-early gene, promotes cell proliferation, migration, and adhesion. Mol. Cell. Biol. **16:**1326–1334.
29. **Kwee, L., H. S. Baldwin, H. M. Shen, C. L. Stewart, C. Buck, C. A. Buck, and M. A. Labow.** 1995. Defective development of the embryonic and extraembryonic circulatory systems in vascular cell adhesion molecule (VCAM-1) deficient mice. Development **121:**489–503.
30. **Latinkic, B. V., F.-E. Mo, J. A. Greenspan, N. G. Copeland, D. J. Gilbert, N. A. Jenkins, and L. F. Lau.** 2001. Promoter function of the angiogenic inducer *Cyr61* gene in transgenic mice: tissue specificity, inducibility during wound healing, and role of the serum response element. Endocrinology **142:**2549–2557.
31. **Latinkic, B. V., T. P. O'Brien, and L. F. Lau.** 1991. Promoter function and structure of the growth factor-inducible immediate early gene *cyr61*. Nucleic Acids Res. **19:**3261–3267.
32. **Lau, L. F., and S. C. Lam.** 1999. The CCN family of angiogenic regulators: the integrin connection. Exp. Cell Res. **248:**44–57.

32a. **Leu, S.-J., S. C. T. Lam, and L. F. Lau.** Proargiogenic activities of CYR61 (CCN1) mediated through integrins αvβ3 and α6β1 in human umbilical vein endothelial cells. J. Biol. Chem., in press.

33. **Li, E., T. H. Bestor, and R. Jaenisch.** 1992. Targeted mutation of the DNA methyltransferase gene results in embryonic lethality. Cell **69:**915–926.
34. **Maisonpierre, P. C., C. Suri, P. F. Jones, S. Bartunkova, S. J. Wiegand, C. Radziejewski, D. Comption, J. McClain, T. H. Aldrich, N. Papadopoulos, T. J. Daly, S. Davis, T. N. Sato, and G. D. Yancopoulos.** 1997. Angiopoietin-2, a natural antagonist for Tie2 that disrupts in vivo angiogenesis. Science **277:**55–60.
35. **O'Brien, T. P., and L. F. Lau.** 1992. Expression of the growth factor-inducible immediate early gene *cyr61* correlates with chondrogenesis during mouse embryonic development. Cell Growth Differ. **3:**645–654.
36. **O'Brien, T. P., G. P. Yang, L. Sanders, and L. F. Lau.** 1990. Expression of *cyr61*, a growth factor-inducible immediate-early gene. Mol. Cell. Biol. **10:** 3569–3577.
37. **Perbal, B.** 2001. NOV (nephroblastoma overexpressed) and the CCN family of genes: structural and functional issues. Mol. Pathol. **54:**57–79.
38. **Risau, W.** 1997. Mechanisms of angiogenesis. Nature **386:**671–674.
39. **Rossant, J., and J. C. Cross.** 2001. Placental development: lessons from mouse mutants. Nat. Rev. Genet. **2:**538–548.
40. **Ryseck, R.-P., H. Macdonald-Bravo, M.-G. Mattei, and R. Bravo.** 1991. Structure, mapping, and expression of *fisp-12*, a growth factor-inducible gene encoding a secreted cysteine-rich protein. Cell Growth Differ. **2:**225–233.
41. **Sampath, D., R. C. Winneker, and Z. Zhang.** 2001. Cyr61, a member of the CCN family, is required for MCF-7 cell proliferation: regulation by 17beta-estradiol and overexpression in human breast cancer. Endocrinology **142:** 2540–2548.
42. **Schober, J. M., N. Chen, T. M. Grzeszkiewicz, E. E. Emeson, T. P. Ugarova, R. D. Ye, L. F. Lau, and S. C. T. Lam.** 2002. Identification of integrin αMβ2 as an adhesion receptor on peripheral blood monocytes for Cyr61 (CCN1) and connective tissue growth factor (CCN2): immediate-early gene products expressed in atherosclerotic lesions. Blood **99:**4457–4465.
43. **Schreiber, J., E. Riethmacher-Sonnenberg, D. Riethmacher, E. E. Tuerk, J. Enderich, M. R. Bösl, and M. Wegner.** 2000. Placental failure in mice lacking

the mammalian homolog of glial cells missing, GCMa. Mol. Cell. Biol. **20:**2466–2474.
44. **Stupack, D. G., and D. A. Cheresh.** 2002. ECM remodeling regulates angiogenesis: endothelial integrins look for new ligands. Sci. Signal Transduction Knowledge Environ. **2002:**PE7.
45. **Su, F., M. Overholtzer, D. Besser, and A. J. Levine.** 2002. WISP-1 attenuates p53-mediated apoptosis in response to DNA damage through activation of the Akt kinase. Genes Dev. **16:**46–57.
46. **Suri, C., P. F. Jones, S. Patan, S. Bartunkova, P. C. Maisonpierre, S. Davis, T. N. Sato, and G. D. Yancopoulos.** 1996. Requisite role of angiopoietin-1, a ligand for the TIE-2 receptor, during embryonic angiogenesis. Cell **87:**1171–1180.
47. **Tsai, M. S., A. E. Hornby, J. Lakins, and R. Lupu.** 2000. Expression and function of CYR61, an angiogenic factor, in breast cancer cell lines and tumor biopsies. Cancer Res. **60:**5603–5607.
48. **Wong, M., M. L. Kireeva, T. V. Kolesnikova, and L. F. Lau.** 1997. Cyr61, product of a growth factor-inducible immediate-early gene, regulates chondrogenesis in mouse limb bud mesenchymal cells. Dev. Biol. **192:**492–508.
49. **Xie, D., C. W. Miller, J. O'Kelly, K. Kakachi, A. Sakashita, J. W. Said, J. Gornbein, and H. P. Koeffler.** 2001. Breast cancer: Cyr61 is over-expressed, estrogen inducible and associated with more advanced disease. J. Biol. Chem. **276:**14187–14194.
50. **Yancopoulos, G. D., S. Davis, N. W. Gale, J. S. Rudge, S. J. Wiegand, and J. Holash.** 2000. Vascular-specific growth factors and blood vessel formation. Nature **407:**242–248.
51. **Yang, G. P., and L. F. Lau.** 1991. Cyr61, product of a growth factor-inducible immediate early gene, is associated with the extracellular matrix and the cell surface. Cell Growth Differ. **2:**351–357.
52. **Yang, J. T., H. Rayburn, and R. O. Hynes.** 1995. Cell adhesion events mediated by alpha 4 integrins are essential in placental and cardiac development. Development **121:**549–560.